Published in final edited form as:
Bone. 2013 January ; 52(1): 93–101. doi:10.1016/j.bone.2012.09.011.

Adherent Lipopolysaccharide Inhibits the Osseointegration of Orthopaedic Implants by Impairing Osteoblast Differentiation

Lindsay A. Bonsignore, BS[1,2], **J. Robert Anderson, MD**[1], **Zhenghong Lee, PhD**[3], **Victor M. Goldberg, MD**[1], and **Edward M. Greenfield, PhD**[1,2,4]

[1]Department of Orthopaedics, Case Western Reserve University, Cleveland, OH

[2]Department of Pathology, Case Western Reserve University, Cleveland, OH

[3]Department of Radiology, Case Western Reserve University, Cleveland, OH

[4]National Center for Regenerative Medicine, Case Western Reserve University, Cleveland, OH

Abstract

Osseointegration is the process by which an orthopaedic implant makes direct bone-to-implant contact and is crucial for the long-term function of the implant. Surface contaminants, such as bacterial debris and manufacturing residues, may remain on orthopaedic implants after sterilization and impair osseointegration. For example, specific lots of implants that were associated with impaired osseointegration and high failure rates were discovered to have contaminants including bacterial debris. Therefore, the goals of this study were to determine if bacterial debris exists on sterile orthopaedic implants and if adherent bacterial debris inhibits the osseointegration of orthopaedic implants. We found that debris containing lipopolysaccharide (LPS) from Gram-negative bacteria exists on both sterile craniofacial implants and wrist implants. Levels of bacterial debris vary not only between different lots of implants but within an individual lot. Using our murine model of osseointegration, we found that ultrapure LPS adherent to the implants inhibited bone-to-implant contact and biomechanical pullout measures. Analysis of osseointegration in knock-out mice demonstrated that adherent LPS inhibited osseointegration by signaling through its primary receptor, Toll-like receptor 4, and not by signaling through Toll-like receptor 2. Ultrapure LPS adherent to titanium alloy discs had no detectable effect on early stages of MC3T3-E1 osteogenesis *in vitro* such as attachment, spreading or growth. However, later stages of osteogenic differentiation and mineralization were inhibited by adherent LPS. Thus, LPS may inhibit osseointegration in part through cell autonomous effects on osteoblasts. These results highlight bacterial debris as a type of surface contaminant that can impair the osseointegration of orthopaedic implants.

Keywords

orthopaedic implants; osseointegration; osteoblasts; bacterial debris; lipopolysaccharide

Corresponding Author: Edward Greenfield, Department of Orthopaedics, Case Western Reserve University, 2109 Adelbert Road, Biomedical Research Building Room 331, Cleveland, OH 44106, Phone# 1-216-368-1331, Fax# 1-216-368-1332, Edward.greenfield@case.edu.

1. Introduction

Clinical success of orthopaedic implants depends upon two main factors: initial fixation due to osseointegration in the first few months and maintenance of the fixation over the long term [1]. Osseointegration is the process by which an orthopaedic implant develops stable fixation through direct bone-to-implant contact [2, 3]. The events necessary for osseointegration include mesenchymal cell attachment, spreading, proliferation and differentiation into matrix-secreting osteoblasts on the implant surface that results in the formation of mineralized bone around the implant [4]. Osseointegration provides a biomechanically stable environment in which the implant can persist under conditions of normal loading [2, 5]. Impaired osseointegration can lead to an increased risk of subsequent loosening due to micromotion [6] and/or wear particle migration along the implant which can enhance particle-mediated osteolysis [7]. Therefore, osseointegration is associated with high success rates and is crucial for the implant's long-term function.

Surface contaminants that remain on sterilized medical devices may have pathophysiological effects in the body and affect the function of the device. Contaminants, including bacterial debris and manufacturing residues, can remain on orthopaedic implants and other medical devices after sterilization procedures such as autoclaving [8–13]. Bacterial debris contaminants include pathogen-associated molecular patterns (PAMPs) that can activate the immune system. The best characterized PAMP, lipopolysaccharide (LPS), is derived from Gram-negative bacteria, is ubiquitous, has a high affinity for biomaterial surfaces [14], and is resistant to removal by sterilization [15]. LPS induces inflammatory pathophysiological responses by activating Toll-like Receptor 4 (TLR4), which is expressed by most mammalian cell types [16]. Signaling through TLR4 results in innate immune responses such as inflammatory cytokine production [17]. Other common bacterial-derived debris that induce similar inflammatory effects include lipoteichoic acids from Gram-positive bacteria and lipopeptides and peptidoglycans derived from both Gram-positive and Gram-negative bacteria [18].

The US Food and Drug Administration (FDA) guidelines require medical device manufacturers to test for the Gram-negative bacterial debris, LPS, by immersing medical devices in water and then measuring the eluted LPS [19]. However, water elution of LPS is inefficient [14, 15, 20]. Considerable amounts of LPS may therefore adhere to the surface of a medical device despite low levels in the eluate. For example, adherent LPS exists on discs made of titanium or titanium alloy that were produced, grit-blasted, cleaned, passivated, packaged and sterilized by a major orthopaedic implant manufacturer using procedures identical to those used for actual implants [15]. In addition, specific lots of implants that were associated with early failure rates were found to be contaminated with LPS and machine oil [21]. Failed implants lacked fixation and had a severe inflammatory response, but did not have any evidence of clinical infection [22]. Bacterial debris on implants may inhibit osseointegration because soluble LPS and Pam3Cys, a synthetic lipopeptide known to activate TLR2, inhibit osteoblast differentiation in cell culture [23–27]. LPS adherent to titanium and titanium alloy surfaces does not affect osteoblast attachment but that study did not examine osteogenic differentiation or mineralization [28].

We, therefore, hypothesized that bacterial debris exists on sterile orthopaedic implants, and that adherent bacterial debris inhibits the osseointegration of orthopaedic implants. To test the hypothesis that bacterial debris exists on orthopaedic implants, we measured LPS directly on two different types of sterile clinical implants by complete immersion of the implants in the LPS assay solution. To test the hypothesis that adherent bacterial debris inhibits the osseointegration of orthopaedic implants, we examined the effect of LPS

adherent to titanium alloy surfaces *in vivo* using our murine osseointegration model [12] and *in vitro* using MC3T3-E1 pre-osteoblast cells.

2. Materials and Methods:

2.1 Implants

Titanium alloy wrist screw implants were received from Hand Innovations (Distal Radius Fracture Repair Set, Locking Screws, Depuy, Warsaw, IN). Wrist implants are 2.2 mm in diameter and 28 mm in length. Implants were either smooth or threaded at the tip. Wrist implants were either autoclaved one time (132°C for eight minutes followed by a twenty minute dry cycle; sterilization recommended by manufacturer before surgical implantation) or were from a surgical kit that had undergone greater than twenty cycles of autoclaving between uses in the operating room.

Craniofacial titanium alloy screw implants, lot #30321493, lot #30268178, lot #1027470 and lot#31791566 were received from KLS Martin (Catalog# 25-660-02, Jacksonville, FL). Craniofacial implants are self-tapping and measure 1 mm in diameter and 2 mm in length. Implants were autoclaved at 134°C for eight minutes followed by a thirty minute dry cycle. This sterilization process is recommended by the manufacturer before surgical implantation. Following autoclaving, a subset of craniofacial implants were rigorously cleaned with five alternating treatments of alkali ethanol (0.1 N NaOH and 95% ethanol at 32°C) and 25% nitric acid, as we have previously described [12, 15]. LPS was then adhered to a subset of the rigorously cleaned implants by incubation with the indicated concentrations of ultrapure LPS (*E. coli* 0111:B4, InvivoGen, San Diego, CA) in phosphate buffered saline (PBS, CellGro, Manassas, VA) with penicillin-streptomycin (CellGro) for four days followed by extensive washing in PBS with penicillin-streptomycin to remove unbound LPS.

Adherent LPS was directly measured on implants by complete immersion in the Endpoint Chromogenic Limulus Amebocyte Lysate (LAL) assay (QCL-1000, Lonza, Basel, Switzerland) with the addition of β-glucan blocker to prevent false positives due to β-glucan-like molecules [29]. Levels of adherent LPS are reported in Endotoxin Units (EU) per m^2 of surface area as calculated in *Section 2.2*.

2.2 Calculation of Implant Surface Areas

Radiographic images of the implants were taken using a special planar x-ray system that was developed by Thomas Jefferson National Lab (Newport News, VA) and Case Western Reserve University. The digital data acquisition allows a spatial resolution of 50 μm, which provided a clear body silhouette of the implants. Perfect rotational symmetry was assumed and small surface rings were diametrically determined from the silhouette in the horizontal direction. The surface area was then calculated by incrementally integrating these rings in the vertical direction. The thread of the screw is spirally rotational; however, this is negligible for this application because the summed error of the whole surface area calculation is only a small fraction of the surface area in one rotation of the thread. The surface area for the smooth and threaded hand implants was determined to be 199 mm^2 and 205 mm^2, respectively. The surface area of the craniofacial screws was 8.4 mm^2.

2.3 Animals and Surgical Procedure

The experimental protocol was approved by the Case Western Reserve University School of Medicine Institutional Animal Care and Use Committee. Wild-type C57BL/6J mice were obtained from Jackson Laboratories (Bar Harbor, ME). $TLR4^{-/-}$ mice and $TLR2^{-/-}$ mice were obtained from S. Akira [30] and $TLR4^{-/-}$;$TLR2^{-/-}$ mice were obtained from A. Hise [31, 32]. Mouse genotypes were confirmed by PCR of genomic DNA isolated from tail

clips. Knock-out mice were matched for age (6–7 weeks), gender (male) and genetic background (C57Bl/6J). All animals were maintained at the Animal Resource Center of Case Western Reserve University. Animals were fed irradiated ProLab IsoPro RMH 3000 5p76 (PMI Nutritional International, St. Louis, MO) and water ad libitum. Mice were randomly assigned to receive rigorously cleaned implants or implants with the indicated concentrations of adherent LPS. Implants were placed into the anterior diaphysis of the femur as we previously described [12]. The mice tolerated the surgery well and showed no sign of inflammation or infection after surgery or at the time of sacrifice. Mice were sacrificed at one to four weeks following implantation for histomorphometric or biomechanical analysis.

2.4 Histomorphometric Analysis

Histological preparation was performed in the Case Western Reserve University Department of Orthopaedic's Hard Tissue Histology Core Facility as we have previously described [12]. Briefly, cross-sections were cut from undecalcified specimens at a thickness of 200 μm, followed by polishing to approximately 100 μm. Sections were stained with Sanderson's Rapid Bone Stain (Surgipath Medical Industries, Richmond, IL) with an acid fuchsin counterstain. The percentage of bone-to-implant contact (BIC) and the percentage of peri-implant bone were measured by a blinded observer (100X, Leica DMIRB, Wetzlar, Germany) using ImageJ analysis software [12].

2.5 Biomechanical Analysis

Biomechanical pullout testing was performed as previously described [12], except a Test Resources 100R Series Single Column Frame (Test Resources, Shakopee, MN) with a 100R Controller was used. Briefly, femora were placed under wire loops embedded in poly-methyl-methacrylate and the implant was gripped by a custom designed jig [12], which was then attached to the Test Resources Frame. Force was measured through a 10 lb capacity load cell and testing was performed at a displacement rate of 1 mm per minute. Ultimate force, stiffness and work to failure were determined from the resultant load versus displacement curves according to ASTM standards (F543-07).

2.6 Titanium Alloy Discs

Ti – 6Al – 4V discs (titanium alloy, Grade 5, ELI Bar, ASTM F136) were received from Titanium Industries (Wood Dale, IL). Discs are 12.5 mm in diameter and 4 mm in height. Titanium alloy discs were rigorously cleaned with five alternating treatments of alkali ethanol and 25% nitric acid [15]. Ultrapure LPS was then adhered to a subset of the rigorously cleaned discs as described in *Section 2.1.* Adherent LPS was measured on a random sampling of discs using the LAL assay as described in *Section 2.1* [29]. Levels of adherent LPS are reported in EU per m^2 of surface area.

2.7 Cell Culture

MC3T3-E1 pre-osteoblast cells were maintained in minimum essential media (Thermo Scientific Hyclone, Logan, UT) with 10% fetal bovine serum (Hyclone), L-glutamine (CellGro), non-essential amino acids (CellGro) and penicillin-streptomycin. Cells were seeded on titanium alloy discs at 2.5×10^4 cells/cm^2 in alpha minimum essential media (Thermo Scientific Hyclone) with 10% fetal bovine serum, L-glutamine and antibiotic/antimycotic (Invitrogen, Carlsbad, CA). Media was replaced every three days with differentiation media, which consisted of the media described above supplemented with 50 μg/ml ascorbate (Gibco, Grand Island, NY) and 5 mM beta-glycerophosphate (Sigma, St. Louis, MO).

2.8 Cellular Spreading

Discs were rinsed twice with PBS and cells were fixed in 10% formalin for ten minutes. Cells were then permeabilized with 0.1% Triton X-100 in PBS for five minutes. Permeabilized cells were incubated with Texas Red X phalloidin (5 U/ml, Molecular Probes Invitrogen, Eugene, OR) for twenty minutes in the dark and then with 4'-6-diamidino-2-phenylidole dihydrochloride (DAPI, 300 nM, Molecular Probes) for five minutes in the dark. Cells were viewed using a fluorescence microscope (Leica DM6000, 546/12 nm excitation and 600/40 nm emission filters for Texas Red X phalloidin, 360/40 nm excitation and 470/40 nm emission filters for DAPI).

2.9 DNA Quantification and Alkaline Phosphatase Activity

Cell lysates were harvested using 2% Triton X-100 and DNA was quantified using PicoGreen dsDNA Quantitation reagent (Molecular Probes) as recommended by the manufacturer. Briefly, cell lysates were diluted in Tris-EDTA buffer (100 or 250 fold for samples harvested, respectively, one or eight days after plating), incubated with an equal volume of PicoGreen dsDNA Quantitation reagent, and the fluorescence was measured (485/20 nm excitation and 528/20 nm emission filters). DNA concentrations were calculated using a standard curve of calf thymus DNA (Sigma). Alkaline phosphatase activity was measured by incubating equal volumes of the cell lysates and 1 mg/ml ρ-nitrophenolphosphate (Sigma) in 1.5 M Tris-HCL buffer containing 1 mM $MgCl_2$ and 1 mM $ZnCl_2$, pH 9. Samples were incubated in the dark for thirty minutes prior to absorbance determination at 410 nm. Alkaline phosphatase activity was calculated using a standard curve of ρ-nitrophenol (Sigma).

2.10 Quantification of mRNA

Isolation of mRNA was performed using the SV Total RNA Isolation System (Promega, Fitchburg, WI), as recommended by the manufacturer. cDNA was synthesized using the SuperScript First-Strand System (Invitrogen). Quantitative RT-PCR was performed with SYBR green PCR Master Mix (BioRad, Hercules, CA) and the 7500 Real-Time PCR Systems and Sequence Detection Software (Applied Biosystems, Carlsbad, CA). Primers (Operon, Huntsville, AL) were designed to overlap exon-exon borders using Primer 3 v 0.4.0 [33]. Primers sequences for runx2, alkaline phosphatase, osterix, and GAPDH are listed in Supplementary Table I. Gene expression was analyzed using a standard curve as we have previously described [34]. All real-time PCR assays included analysis of melting curves [35] and agarose gel electrophoresis to confirm the presence of single PCR reaction products. The identity of real-time PCR products was confirmed by sequencing (Biotic Solutions, New York, NY).

2.11 Mineralization

Media was replaced every three days with differentiation media further supplemented with 50 ng/ml recombinant human bone morphogenetic protein 2 (BMP-2, R&D Systems, Minneapolis, MN). Thirty days after plating, cells were incubated with 20 μM xylenol orange (Sigma) in differentiation media [36]. The next day, xylenol orange staining was viewed using a fluorescence stereomicroscope (Leica MZ16 F, 546/12 nm excitation and 600/40 nm emission filters) and the percentage of surface area mineralized was calculated using ImageJ analysis software.

2.12 Statistical analysis

All statistical analysis was performed using SigmaStat Software 3.0 (Systat Software, San Jose, CA). Data sets that passed normality (Kolmogorov-Smirnov test with Lilliefors' correction) and equal variance testing (Levene median test) were analyzed parametrically by

student's t-tests for pairs of groups and by One-Way or Two-Way ANOVA followed by Bonferroni post-hoc tests for multiple groups. Data sets that failed normality or equal variance testing were analyzed non-parametrically by Mann-Whitney Rank sum tests for pairs of groups and by Kruskal-Wallis One-Way ANOVA on Ranks followed by Dunn's post-hoc tests for multiple groups. Each group included eight to eleven mice for *in vivo* studies and three to four independent experiments for *in vitro* studies. The specific statistical test used and sample size for each group are listed in the figure captions. Results are shown as mean ± standard error unless otherwise noted.

3. Results

To test the hypothesis that adherent bacterial debris exists on sterile orthopaedic implants, we measured adherent LPS derived from Gram-negative bacteria. LPS was measured on two different types of implants used clinically: craniofacial implants and wrist implants. This study focused on those small orthopaedic implants since immersion of large implants in the LPS assay would require excessive amounts of extremely costly reagents. Prior to assay, both craniofacial and wrist implants were autoclaved, which is the sterilization method recommended by the manufacturers before surgical implantation. The level of bacterial debris on the craniofacial implants varied within an individual lot. For example, within lot#30321493 there was a 25 fold difference between the two implants with the highest level of adherent bacterial debris and the two implants with the lowest level (Figure 1A). Because of this variability, individual data points and medians are shown in Figure 1 rather than means and standard deviations. To facilitate comparisons, Figure 1A includes levels of bacterial debris on two lots of craniofacial implants that were previously examined [12] and two new lots of craniofacial implants. This analysis shows significant variability between the four different lots of craniofacial implants. Thus, the four different lots had median values of adherent bacterial debris of 389 EU/m^2 (lot#30321493), 78 EU/m^2 (lot#30268178), 2.2 EU/m^2 (lot#1027470), and 16.4 EU/m^2 (lot#31791566). There is therefore, a 175 fold difference in the median values between the lots with the highest and lowest levels of adherent bacterial debris. Significant levels of adherent bacterial debris also existed on wrist implants. The four wrist implants that were assayed had a median level of 28 EU/m^2 of bacterial debris, after one cycle of autoclaving (left side of Figure 1B). We also found that multiple sterilization cycles reduce the level of adherent bacterial debris. Thus, wrist implants that had undergone greater than twenty cycles of autoclaving had significantly less ($p=0.016$) adherent bacterial debris than implants that had been autoclaved one time (2.6 versus 28 EU/m^2, Figure 1B).

To test the hypothesis that adherent bacterial debris inhibits the osseointegration of orthopaedic implants, we compared the integration of rigorously cleaned implants and implants with adherent bacterial-derived ultrapure LPS in our murine model of osseointegration [12]. For this purpose, rigorously cleaned implants were incubated with increasing concentrations of soluble ultrapure LPS, resulting in increasing amounts of adherent LPS on the implants (Supplementary Figure 1A). Ultrapure LPS was utilized in this study because unpurified LPS contains other bacterial components, such as peptidoglycans and lipoproteins that synergistically induce inflammatory responses [37–39]. Similarly, bacterial debris also contains multiple immunostimulatory molecules and is therefore more potent per Endotoxin Unit than ultrapure LPS [37, 40]. Thus, although both bacterial debris and ultrapure LPS are quantified by the same assay in this study, the reported Endotoxin Units are not comparable. To emphasize this point, bacterial debris measurements are reported in standard notation while ultrapure LPS measurements are reported in scientific notation.

Rigorously cleaned implants and implants with adherent LPS were implanted into the femur of mice and osseointegration was analyzed [12]. Histomorphometric measurements of osseointegration of the rigorously cleaned implants (open circles, Figure 2A and 2B) were similar to those we found previously with rigorously cleaned implants at one week after implantation [12]. However, the percentage of bone-to-implant contact (BIC) was inhibited in a dose dependent manner in mice with implants with adherent LPS (filled circles, Figure 2A). Thus, 2×10^2 EU/m^2 of LPS inhibited BIC by 15%, 1.2×10^3 EU/m^2 inhibited by 39% ($p=0.017$), and 1×10^4 EU/m^2 inhibited by 47% ($p=0.003$). Implants with the highest level of adherent LPS were used for all future experiments. Inhibition of BIC by adherent LPS was maintained throughout a four week time course ($p<0.001$, Figure 2C). The impaired BIC with adherent LPS is illustrated in the representative histological cross-sections at one week after implantation shown in Figure 2E. In contrast to the inhibition of BIC, the percentage of peri-implant bone was not affected by adherent LPS (Figure 2B, 2D and 2E, see also Figure 4B and 4C). Inhibition of BIC but not peri-implant bone by adherent LPS is similar to what we have previously found with implants with contaminated surfaces [12]. To further examine the effects of adherent LPS on osseointegration, we performed biomechanical pullout testing at two weeks after implantation. All three biomechanical parameters were inhibited by adherent LPS by approximately 25%. The effect on ultimate force was statistically significant ($p=0.03$, Figure 3A), and there was a statistical trend towards reduced stiffness ($p=0.076$, Figure 3B) and work to failure ($p=0.212$, Figure 3C). The effects of adherent LPS are illustrated in the representative force versus displacement curves in Figure 3D.

We then tested the hypothesis that adherent LPS inhibits osseointegration through its primary receptor, TLR4, by comparing wild-type mice, TLR4$^{-/-}$ mice, TLR2$^{-/-}$ mice, and TLR4$^{-/-}$;TLR2$^{-/-}$ mice. As expected, the rigorously cleaned implants at one week after implantation had similar amounts of osseointegration in all four genotypes (open bars in Figure 4A and 4B). Adherent LPS did not affect BIC in the TLR4$^{-/-}$ mice or the TLR4$^{-/-}$;TLR2$^{-/-}$ mice but inhibition was approximately 37% in both the wild-type mice and the TLR2$^{-/-}$ mice ($p=0.01$ and $p=0.002$ respectively, Figure 4A). These results with adherent LPS are illustrated in the representative histological cross-sections shown in Figure 4C. Therefore, adherent LPS inhibits osseointegration by signaling through its primary receptor, TLR4.

To determine whether adherent LPS can inhibit osseointegration through cell autonomous effects on osteoblast cells, we examined the effect of ultrapure LPS adhered to titanium alloy discs on MC3T3-E1 pre-osteoblast cells *in vitro*. Rigorously cleaned discs were incubated with increasing concentrations of soluble ultrapure LPS, resulting in increasing amounts of LPS adherent to the discs (Supplementary Figure 1B). Adherent LPS had no detectable effect on early stages of osteogenesis including osteoblast attachment as analyzed by DNA measurements at one day, spreading as analyzed by fluorescence images of cells at one day, and growth as analyzed by DNA measurements at eight days (Figure 5A and 5B). Adherent LPS had a modest inhibitory effect on the expression of the early osteoblast differentiation marker, runx2 (Figure 5C). However, this effect was not statistically significant. In contrast, adherent LPS potently inhibited later stages of osteogenic differentiation and mineralization. Thus, adherent LPS significantly inhibited osterix expression at three, six and nine days ($p<0.05$, Figure 5D) and alkaline phosphatase expression at six days ($p<0.05$, Figure 5E). In addition, adherent LPS inhibited alkaline phosphatase activity in a dose dependent manner (Figure 5F). Thus at eight days, 2.7×10^1 EU/m^2 and 1.4×10^2 EU/m^2 of adherent LPS inhibited alkaline phosphatase activity by 13%, 6.4×10^2 EU/m^2 inhibited by 30%, and 2.1×10^4 EU/m^2 inhibited by 62% ($p<0.05$). Adherent LPS also inhibited mineralization in a dose dependent manner (Figure 5G). Accordingly at thirty days, 1×10^2 EU/m^2 of adherent LPS inhibited mineralization by 26%

and 2×10^4 EU/m^2 inhibited by 54% ($p<0.05$). The impaired mineralization with adherent LPS is illustrated in the representative discs stained with xylenol orange shown in Figure 5H.

4. Discussion

Osseointegration is crucial for early fixation as well as long-term success of orthopaedic implants. Contaminants, such as bacterial debris, may remain on an implant surface after sterilization procedures and inhibit osseointegration [12]. The goals of this study were, therefore, to determine if bacterial debris exists on sterile orthopaedic implants and if adherent bacterial debris inhibits the osseointegration of orthopaedic implants. We found that variable levels of Gram-negative bacterial debris exist on both craniofacial implants and wrist implants. Using our murine model of osseointegration, we also found that bacterial-derived ultrapure LPS on implants inhibited the histomorphometric measure of bone-to-implant contact (BIC) and biomechanical pullout measures. In contrast, the percentage of peri-implant bone was not affected by adherent LPS. This pattern of effects by adherent LPS is similar to what we have previously found with implants with contaminated surfaces [12]. Analysis of osseointegration in knock-out mice demonstrated that adherent LPS on implants inhibited osseointegration by signaling through its primary receptor, TLR4. Ultrapure LPS adherent to titanium alloy discs had no detectable effect on early stages of MC3T3-E1 osteogenesis *in vitro* such as attachment, spreading or growth. However, later stages of osteogenic differentiation and mineralization were inhibited by adherent LPS. Thus, adherent LPS may inhibit osseointegration in part through cell autonomous effects on osteoblasts.

The FDA limit for bacterial debris on implantable medical devices is 20 EU/device. Medical device manufacturers measure adherent bacterial debris by measuring eluted LPS in water washes. However, water elution of LPS is inefficient [14, 15, 20], therefore, manufacturers likely underestimate the levels of bacterial debris on their devices. In this study, bacterial debris was measured directly on the implants by complete immersion in the LPS assay. Nonetheless, all of the implants with adherent ultrapure LPS used in this study would pass the FDA guideline of 20 EU/device. It is inappropriate to compare levels of bacterial debris on the autoclaved clinical implants with levels on implants with ultrapure LPS, because ultrapure LPS is substantially less potent than bacterial debris (see *Section 3*).

We found that multiple cycles of autoclaving significantly reduced the level of bacterial debris on implants compared to a single autoclave cycle. These results are reminiscent of our previous finding that multiple cycles of alternating alkali ethanol and nitric acid are more effective at removing bacterial debris than one cycle [15]. Autoclaving relies on pressurized steam for sterilization, and a single standard cycle (132–134°C for eight minutes) is relatively ineffective at removing adherent bacterial debris [41, 42]. For example, 180°C for more than three hours or 250°C for more than thirty minutes is required to effectively destroy LPS [42]. The results of this study provide rationale for future studies to determine whether multiple sterilization cycles improve osseointegration of implants.

A limitation of our study is that although the craniofacial implants and wrist implants are used clinically, they do not rely on osseointegration for function. Additionally most osseointegrated implants are sterilized by the manufacturer, while the implants we studied are sterilized at the hospital before use. However, this study focused on small implants since immersion of large osseointegrated implants in the LPS assay would require excessive amounts of extremely costly reagents. Nonetheless, the levels of bacterial debris on craniofacial and wrist implants are similar to the levels that we previously found on discs made of implant material that were produced, grit-blasted, cleaned, passivated, packaged

and sterilized by a major manufacturer of orthopaedic implants exactly as it processes actual implants (15 ± 2.4 EU/m^2) [15]. The levels of adherent bacterial debris varied significantly between the four lots of craniofacial implants. Interestingly, levels of bacterial debris also varied within individual lots, most notably on craniofacial implant lot #30321493. This variability may be important because the FDA requires that medical device manufacturers test for bacterial debris only on a small subset of devices from each lot [19]. Therefore, levels of bacterial debris on the samples tested may not necessarily reflect the levels on the other devices in that lot. Implants with higher levels of bacterial debris may have impaired integration, as we found that adherent LPS on implants inhibits BIC and biomechanical measures of osseointegration.

One limitation of our murine osseointegration model used in this study is that mice have lower mechanical loads supporting their bones and a higher potential for bone regeneration than larger animals such as humans. In addition, the implant in our model is under non-loading conditions. Despite these limitations, our murine model of osseointegration provides significant advantages [12] and is appropriate for examining certain types of questions, not related to mechanical loading, such as whether adherent LPS inhibits osseointegration. Also, non-loading models are useful for examining the effects of materials, coating, surface modifications, or the effects of surface contaminants on osseointegration before testing in a loading model.

Analysis of osseointegration in knock-out mice demonstrated that adherent LPS on implants inhibited osseointegration by signaling through TLR4, and not by signaling through TLR2. In addition to recognizing PAMPs, TLRs are also receptors for endogenous molecules known as alarmins or endogenous danger-associated molecular patterns [43, 44]. Our results support the conclusion that alarmins are not sufficient to activate TLRs during osseointegration, and that cognate PAMPs are required. If this were not the case, then non-cognate TLRs would contribute to inhibition of osseointegration by adherent LPS. However, we found that LPS acts through its cognate receptor TLR4 and that TLR2 does not contribute. These results are similar to our previous finding that cognate PAMPs are required to activate TLRs during osteolysis induced by orthopaedic wear particles, and that alarmins are not sufficient [32]. Future studies using knock-out mice will be performed to determine if adherent bacterial debris on autoclaved clinical implants inhibits osseointegration through TLRs.

One potential mechanism by which adherent bacterial debris may inhibit osseointegration is through cell autonomous effects on osteoblast cells and their precursors. We found that ultrapure LPS adherent to titanium alloy discs inhibited differentiation and mineralization but had no effect on attachment, spreading or growth of MC3T3-E1 pre-osteoblast cells *in vitro*. These results are similar to a number of studies that showed soluble LPS had no effect on osteoblast growth but inhibited later stages of osteogenic differentiation and mineralization on tissue culture plastic [23–26]. In addition, one study found that LPS adherent to titanium and titanium alloy surfaces did not affect MC3T3-E1 cell attachment [28]. However, that study did not examine effects on osteogenic differentiation or mineralization. Also consistent with our results, Bandow et al. demonstrated that the inhibitory effect of soluble LPS on osteoblast differentiation is a result of signaling through the myeloid differentiation factor 88 (Myd88) pathway, which is downstream of TLR4 [26]. These results indicate that adherent LPS on implants may inhibit osseointegration in part through cell autonomous effects on osteoblast cells. Alternatively, LPS could also activate inflammatory cells and osteoclasts and thereby contribute to impaired osseointegration.

In conclusion, we found that variable levels of Gram-negative bacterial debris exist on both craniofacial implants and wrist implants. Using our murine model of osseointegration, we

found that bacterial-derived ultrapure LPS on implants inhibits osseointegration through its primary receptor TLR4. Adherent LPS had no effect on early stages of MC3T3-E1 osteogenesis *in vitro.* However, later stages of osteogenic differentiation and mineralization were inhibited by adherent LPS. Thus, adherent LPS may inhibit osseointegration in part through cell autonomous effects on osteoblasts. These results highlight bacterial debris as a type of surface contaminant that can impair the osseointegration of orthopaedic implants. In addition, these results justify the need for the development of better detection and removal techniques for LPS on orthopaedic implants.

Supplementary Material

Refer to Web version on PubMed Central for supplementary material.

Acknowledgments

We thank Depuy/Mitek for the generous gift of the wrist screws, Joscelyn Tatro for assistance with surgeries, Nathan Tinley for help with surface area calculations, Joseph Molter for help with radiography, Sarah McBride for help with image analysis, Christopher Hernandez for help analyzing biomechanical testing results, and Teresa Pizzuto for histological preparation. This work was supported by NIH T32 AR07505 (LAB) and the Harry E. Figgie III MD Professorship (EMG).

References

1. Bauer T, Schils J. The pathology of total joint arthroplasty.II. Mechanisms of implant failure. Skeletal Radiol. 1999; 28:483–497. [PubMed: 10525792]
2. Albrektsson T, Branemark P, Hansson H, Lindstrom J. Osseointegrated titanium implants. Requirements for ensuring a long-lasting, direct bone-to-implant anchorage in man. Acta Orthop Scand. 1981; 52:155–170. [PubMed: 7246093]
3. Branemark P. Osseointegration and its experimental background. J Prosthet Dent. 1983; 50:399–410. [PubMed: 6352924]
4. Puleo D, Nanci A. Understanding and controlling the bone-implant interface. Biomaterials. 1999; 20:2311–2321. [PubMed: 10614937]
5. Branemark R, Branemark P, Rydevik B, Myers R. Osseointegration in skeletal reconstruction and rehabilitation: a review. J Rehabil Res Dev. 2001; 38:175–181. [PubMed: 11392650]
6. Ryd L, Albrektsson B, Carlsson L, Dansgard F, Herberts P, Lindstrand A, Regner L, Toksvig-Larsen S. Roentgen stereophotogrammetric analysis as a predictor of mechanical loosening of knee prostheses. J Bone Joint Surg. 1995; 77B:377–383.
7. Schmalzried T, Jasty M, Harris W. Periprosthetic bone loss in total hip arthroplasty. Polyethylene wear debris and the concept of the effective joint space. J Bone Joint Surg. 1992; 74A:849–863. [PubMed: 1634575]
8. Daniel, A.; Kimmelman, E. The FDA and Worldwide Quality System Requirements Guidebook for Medical Devices. 2nd ed. Milwaukee: ASQ Quality Press; 2008.
9. Spiegelberg, S. How Clean is Clean Enough?. San Antonio: ASTM Workshop of Medical Device Cleanliness; 2010.
10. Spiegelberg, S. ASTM Activities for Assessing Cleanliness of Medical Devices. In: Shrivastava, S., editor. Medical Device Materials. Materials Park: ASM International; 2004. p. 125-126.
11. Arys A, Philippart C, Dourov N, He Y, Le Q, Pireaux J. Analysis of titanium dental implants after failure of osseointegration: combined histological, electron microscopy, and X-ray photoelectron spectroscopy approach. J Biomed Mater Res. 1998; 43:300–312. [PubMed: 9730068]
12. Bonsignore L, Colbrunn R, Tatro J, Messerschmitt P, Hernandez C, Goldberg V, Stewart M, Greenfield E. Surface contaminants inhibit osseointegration in a novel murine model. Bone. 2011; 49:923–930. [PubMed: 21801863]
13. Williams D. Endotoxins and medical devices: the significance of dead bacteria. Med Device Technol. 2003; 14:8–11.

14. Nelson S, Knoernschild K, Robinson F, Schuster G. Lipopolysaccharide affinity for titanium implant biomaterials. J Prosthet Dent. 1997; 77:76–82. [PubMed: 9029469]
15. Ragab A, VanDeMotter R, Lavish S, Goldberg V, Ninomiya J, Carlin C, Greenfield E. Measurement and removal of adherent endotoxin from titanium particles and implant surfaces. J Orthop Res. 1999; 17:803–809. [PubMed: 10632445]
16. Lee M, Kim Y. Signaling pathways downstream of pattern-recognition receptors and their cross talk. Annu Rev Biochem. 2007; 76:447–480. [PubMed: 17328678]
17. Lu Y, Yeh W, Ohashi P. LPS/TLR4 signal transduction pathway. Cytokine. 2008; 42:145–151. [PubMed: 18304834]
18. Zahringer U, Lindner B, Inamura S, Heine H, Alexander C. TLR2 - promiscuous or specific? A critical re-evaluation of a receptor expressing apparent broad specificity. Immunobiology. 2008; 213:205–224. [PubMed: 18406368]
19. US Department of health and human services/Public Health services/Food and Drug Administration. Guideline on validation of the limulus amebocyte lysate test as an end--product endotoxin test for human and animal parenteral drugs, biological products, and medical devices. 1987. p. 1-30.
20. Ross V, Twohy C. Endotoxins and medical devices. Prog Clin Biol Res. 1985; 189:267–281. [PubMed: 4048209]
21. Orthopaedic Device Forum Meeting Summation Report; Bethesda. 2003.
22. Campbell P, Mirra J, Catelas I. Histopathology of tissues from Inter-Op acetabular sockets. Transactions of the Orthopaedic Research Society. 2002; 27:187.
23. Kadono H, Kido J, Kataoka M, Yamauchi N, Nagata T. Inhibition of osteoblastic cell differentiation by lipopolysaccharide extract from Porphyromonas gingivalis. Infect Immun. 1999; 67:2841–2846. [PubMed: 10338489]
24. Loomer P, Ellen R, Tenenbaum H. Characterization of inhibitory effects of suspected periodontopathogen on osteogenesis in vitro. Infect Immun. 1995; 63:3287–3296. [PubMed: 7642257]
25. Xing Q, Ye Q, Fan M, Zhou Y, Xu Q, Sandham A. Porphyromonas gingivalis lipopolysaccharide inhibits the osteoblastic differentiation of preosteoblasts by activating Notch1 signaling. J Cell Physiol. 2010; 225:106–114. [PubMed: 20648628]
26. Bandow K, Maeda A, Kakimoto K, Kusuyama J, Shamoto M, Ohnishi T, Matsuguchi T. Molecular mechanisms of the inhibitory effect of lipopolysaccharide (LPS) on osteoblast differentiation. Biochem Biophys Res Commun. 2010; 402:755–761. [PubMed: 21036155]
27. Pevsner-Fischer M, Morad V, Cohen-Sfady M, Rousso-Noori L, Zanin-Zhorov A, Cohen S, Cohen I, Zipori D. Toll-like receptors and their ligands control mesenchymal stem cell functions. Blood. 2007; 109:1422–1432. [PubMed: 17038530]
28. Nouneh R, Wataha J, Hanes P, Lockwood P. Effect of lipopolysaccharide contamination on the attachment of osteoblast-like cells to titanium and titanium alloy in vitro. J Oral Implantol. 2001; 27:174–179. [PubMed: 12500875]
29. Nalepka J, Greenfield E. Detection of bacterial endotoxin in human tissues. Biotechniques. 2004; 37:413–417. [PubMed: 15470896]
30. Takeuchi O, Hoshino K, Kawai T, Sanjo H, Takada H, Ogawa T, Takeda K, Akira S. Differential roles of TLR2 and TLR4 in recognition of gram-negative and gram-positive bacterial cell wall components. Immunity. 1999; 11:443–451. [PubMed: 10549626]
31. Hise A, Daehnel K, Gillette-Ferguson I, Cho E, McGarry H, Taylor M, Golenbock D, Fitzgerald K, Kazura J, Pearlman E. Innate immune responses to endosymbiotic Wolbachia bacteria in Brugia malayi and Onchocerca volvulus are dependent on TLR2, TLR6, MyD88, and Mal, but not TLR4, TRIF, or TRAM. J Immunol. 2007; 178:1068–1076. [PubMed: 17202370]
32. Greenfield E, Beidelschies M, Tatro J, Goldberg V, Hise A. Bacterial pathogen-associated molecular patterns stimulate biological activity of orthopaedic wear particles by activating cognate Toll-like receptors. J Biol Chem. 2010; 285:32378–32384. [PubMed: 20729214]
33. Rozen, S.; Skaletsky, H. Primer3 on the WWW for general users and for biologist programmers. In: Krawetz, S.; Misener, S., editors. Bioinformatics Methods and Protocols: Methods in Molecular Biology. Totowa: Humana Press; 2000. p. 365-386.

34. Dai J, He P, Chen X, Greenfield E. TNFalpha and PTH utilize distinct mechanisms to induce IL-6 and RANKL expression with markedly different kinetics. Bone. 2006; 38:509–520. [PubMed: 16316790]

35. Giulietti A, Overbergh L, Valckx D, Decallonne B, Bouillon R, Mathieu C. An overview of real-time quantitative PCR: applications to quantify cytokine gene expression. Methods. 2001; 25:386–401. [PubMed: 11846608]

36. Wang Y, Liu Y, Maye P, Rowe D. Examination of mineralized nodule formation in living osteoblastic cultures using fluorescent dyes. Biotechnol Prog. 2006; 22:1697–1701. [PubMed: 17137320]

37. Hirschfeld M, Ma Y, Weis J, Vogel S, Weis J. Cutting edge: repurification of lipopolysaccharide eliminates signaling through both human and murine toll-like receptor 2. J Immunol. 2000; 165:618–622. [PubMed: 10878331]

38. Uehara A, Yang S, Fujimoto Y, Fukase K, Kusumoto S, Shibata K, Sugawara S, Takada H. Muramyldipeptide and diaminopimelic acid-containing desmuramylpeptides in combination with chemically synthesized Toll-like receptor agonists synergistically induced production of interleukin-8 in a NOD2- and NOD1-dependent manner, respectively, in human monocytic cells in culture. Cell Microbiol. 2005; 7:53–61. [PubMed: 15617523]

39. Yang S, Tamai R, Akashi S, Takeuchi O, Akira S, Sugawara S, Takada H. Synergistic effect of muramyldipeptide with lipopolysaccharide or lipoteichoic acid to induce inflammatory cytokines in human monocytic cells in culture. Infect Immun. 2001; 69:2045–2053. [PubMed: 11254557]

40. Kawai T, Akira S. The role of pattern-recognition receptors in innate immunity: update on Toll-like receptors. Nat Immunol. 2010; 11:373–384. [PubMed: 20404851]

41. Williams, K. Depyrogenations Validation, Pyroburden and Endotoxin Removal. In: Williams, K., editor. Endotoxins: Pyrogens, LAL Testing and Depyrogenation. New York: Informa Healthcare USA, Inc.; 2007. p. 301-328.

42. Gorbet M, Sefton M. Endotoxin: the uninvited guest. Biomaterials. 2005; 26:6811–6817. [PubMed: 16019062]

43. Matzinger P. Friendly and dangerous signals: is the tissue in control? Nat Immunol. 2007; 8:11–13. [PubMed: 17179963]

44. Bianchi M. DAMPs, PAMPs and alarmins: all we need to know about danger. J Leukoc Biol. 2007; 81:1–5. [PubMed: 17032697]

Highlights

- Debris containing LPS from Gram-negative bacteria exists on clinical implants
- Levels of bacterial debris vary between different lots of implants and within an individual lot
- Ultrapure LPS adherent to implants inhibited osseointegration through TLR-4
- Ultrapure LPS adherent to titanium alloy discs inhibited MC3T3-E1 differentiation and mineralization *in vitro*
- LPS may inhibit osseointegration in part through cell autonomous effects on osteoblasts

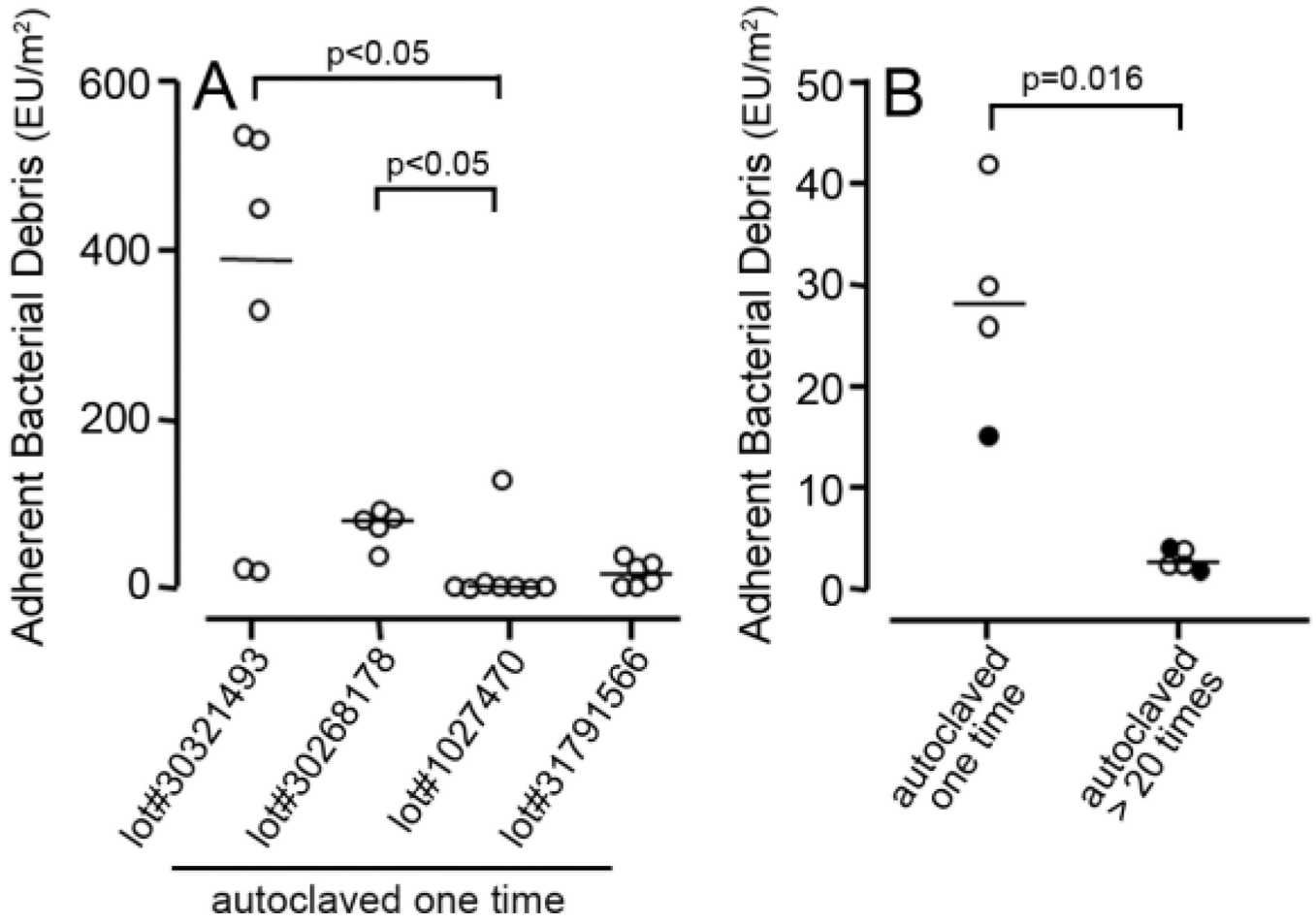

Figure 1. Levels of adherent bacterial debris on sterile clinical implants are highly variable

The level of adherent bacterial debris on four lots of craniofacial implants that had been autoclaved one time (A). lot#30268178 and lot#1027470 were previously examined [12]. The level of adherent bacterial debris on wrist implants that had been autoclaved one time and wrist implants that had undergone greater than twenty cycles of autoclaving (B). Each symbol represents one implant. Horizontal lines denote median values. In B, filled symbols represent smooth wrist implants and open symbols represent threaded wrist implants. EU = Endotoxin Units. Statistical analysis was by One-Way ANOVA on Ranks (A) or Mann-Whitney Rank sum test (B).

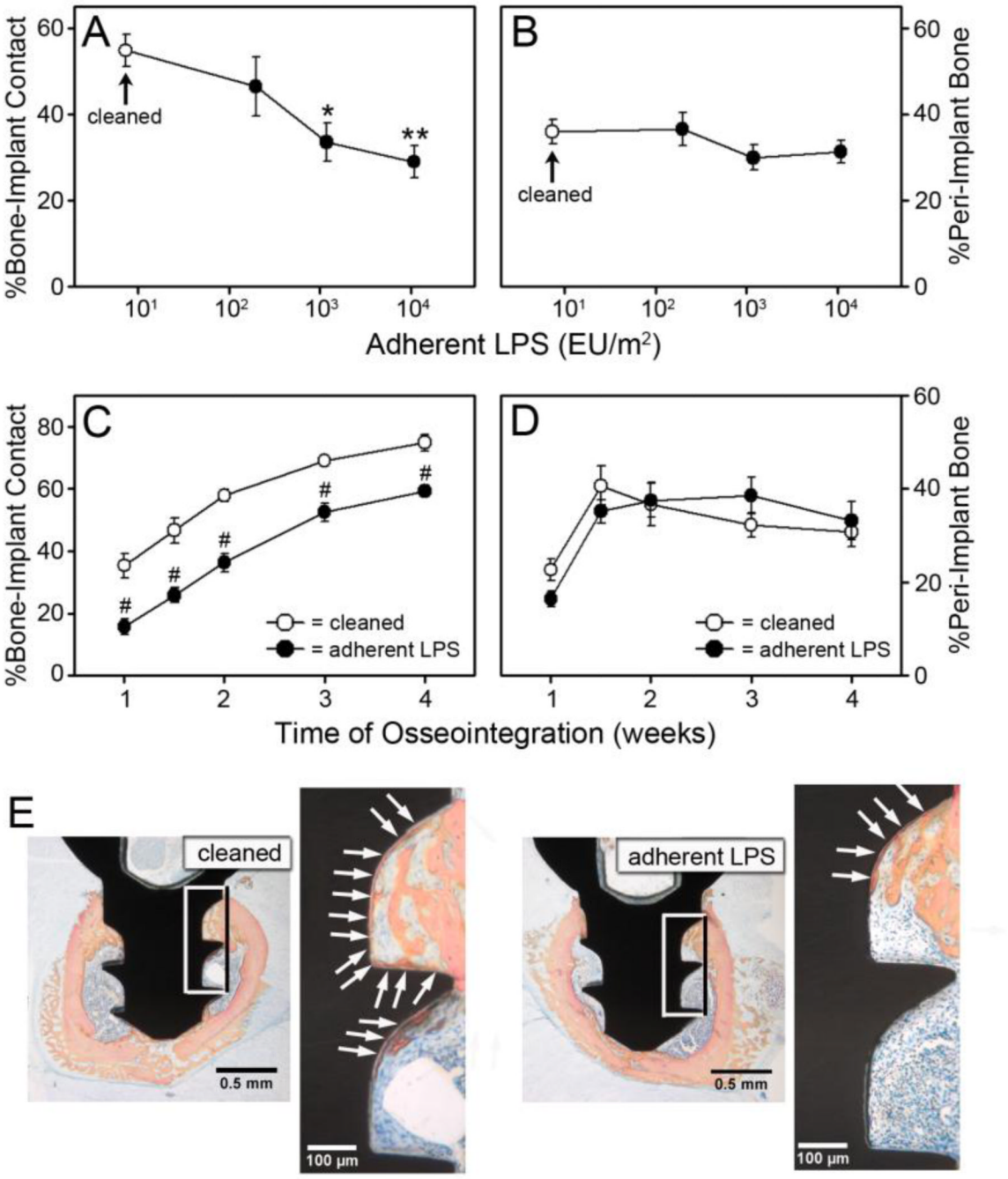

Figure 2. Adherent LPS inhibits bone-to-implant contact

The percentage of bone-to-implant contact (A) and the percentage of peri-implant bone (B) at one week after implantation in wild-type C57Bl/6J mice with rigorously cleaned implants (open circles) or implants with adherent LPS (closed circles). The percentage of bone-to-implant contact (C) and the percentage of peri-implant bone (D) over a four week time course in wild-type C57Bl/6J mice with rigorously cleaned implants (open circles) or implants with 1×10^4 EU/m^2 of adherent LPS (closed circles). Representative histological cross-sections, which are closest to the mean in C, at one week after implantation in mice with rigorously cleaned implants or implants with 1×10^4 EU/m^2 of adherent LPS (E). Boxes indicated area magnified in next panel. Arrows denote bone-to-implant contact.

Statistical analysis was by One-Way ANOVA (A and B) or by Two-Way ANOVA (C and D). * denotes p=0.017, ** denotes p=0.003, and # denotes p<0.001 compared to rigorously cleaned. n=8–11.

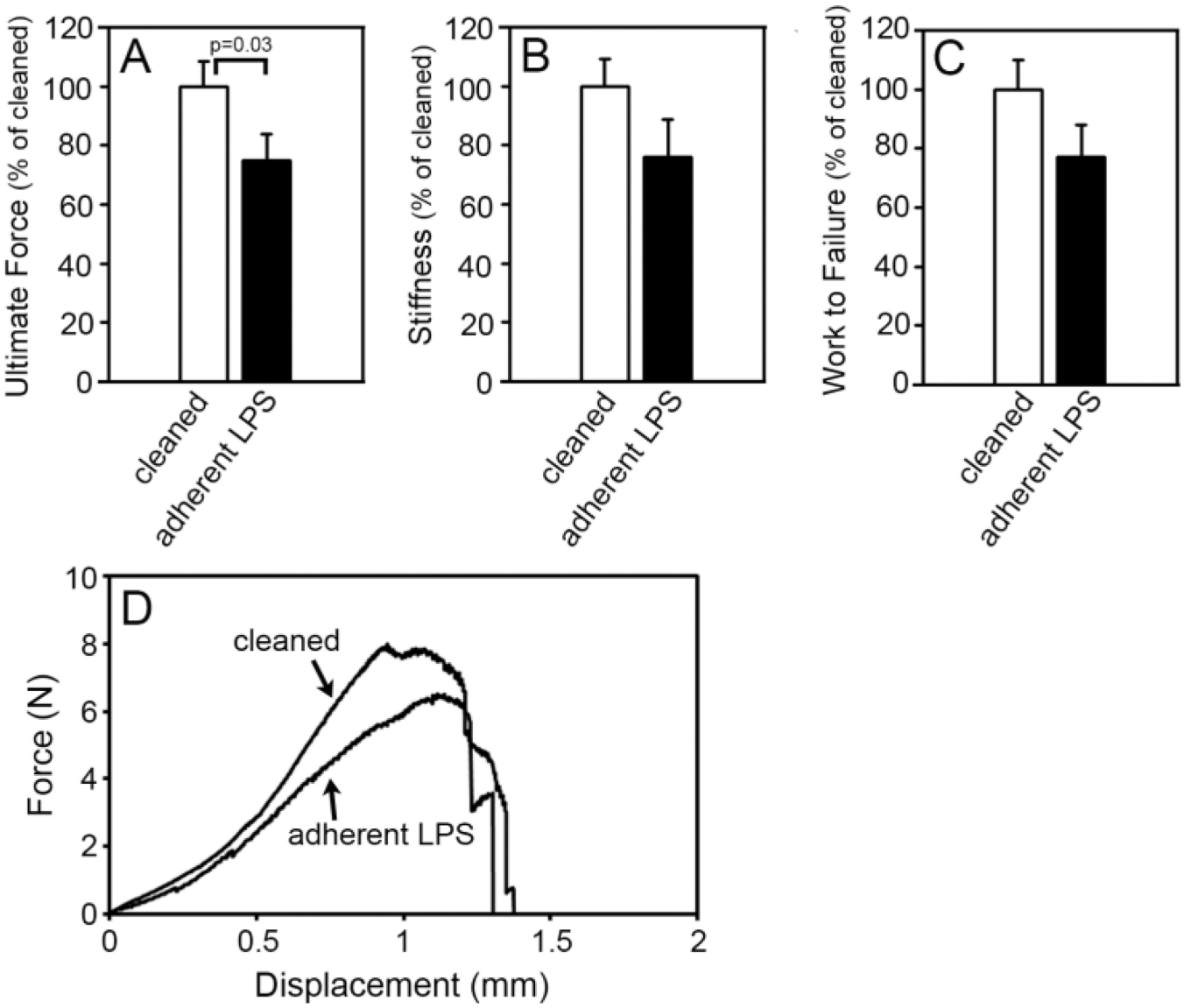

Figure 3. Adherent LPS inhibits biomechanical pullout testing measures

Biomechanical pullout testing measures of ultimate force (A), stiffness (B) and work to failure (C) at two weeks after implantation in wild-type C57BL/6J mice with rigorously cleaned implants (open bars) or implants with 1×10^4 EU/m^2 of adherent LPS (closed bars). Representative force versus displacement curves, which are closest to the mean in A, in mice with rigorously cleaned implants or implants with 1×10^4 EU/m^2 of adherent LPS (D). Results are normalized to the mean value obtained with rigorously cleaned implants. Statistical analysis was by Mann-Whitney Rank sum test. n=11

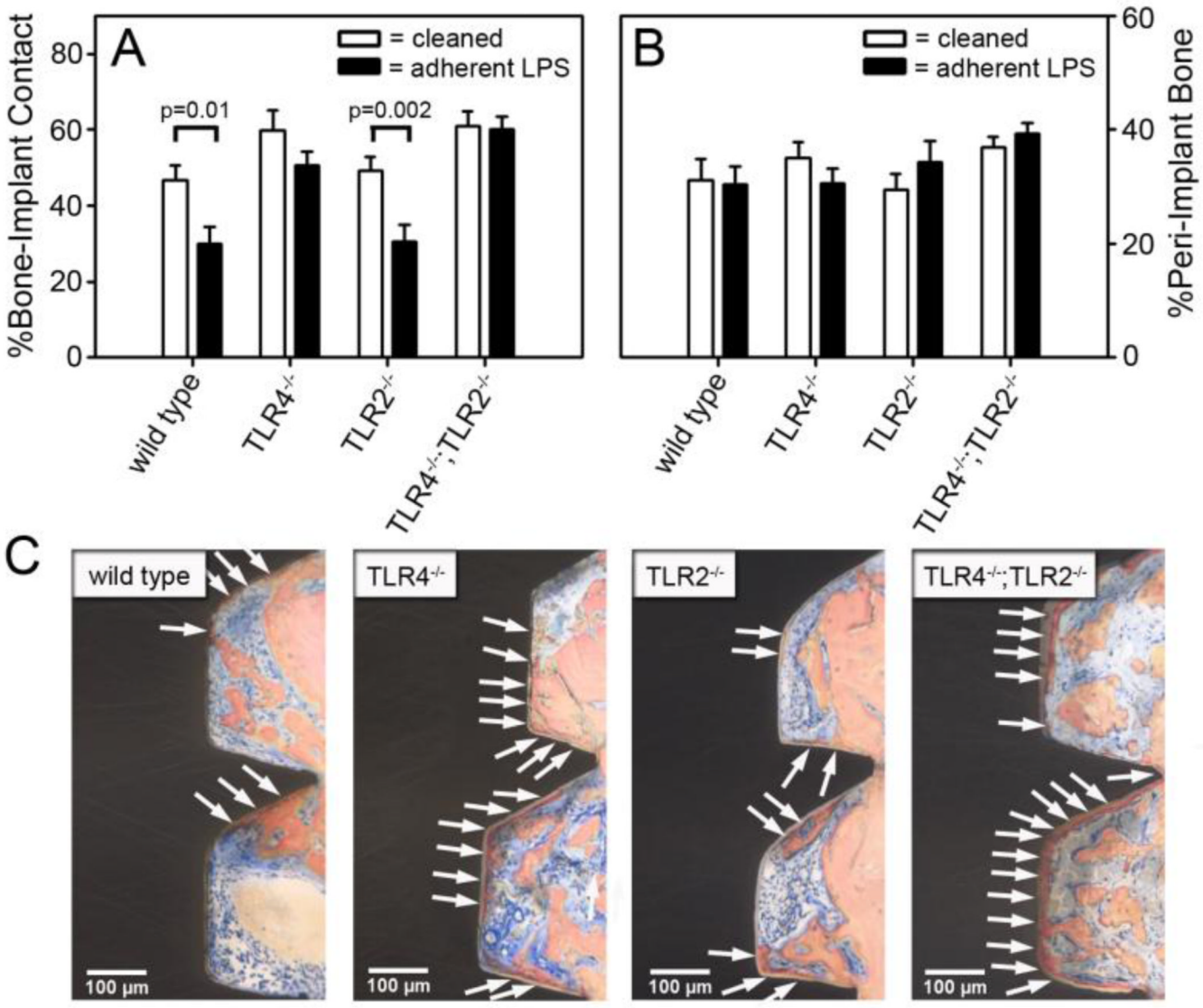

Figure 4. Adherent LPS inhibits bone-to-implant contact through TLR4

The percentage of bone-to-implant contact (A) and the percentage of peri-implant bone (B) in wild-type C57BL/6J mice, $TLR4^{-/-}$ mice, $TLR2^{-/-}$ mice and $TLR4^{-/-};TLR2^{-/-}$ mice one week after implantation with rigorously cleaned implants or implants with 1×10^4 EU/m^2 of adherent LPS. Representative histological cross-sections, which are closest to the mean in A, at one week after implantation in mice with implants with 1×10^4 EU/m^2 of adherent LPS (C). Arrows denote bone-to-implant contact. Statistical analysis was by Two-Way ANOVA. n=8–10.

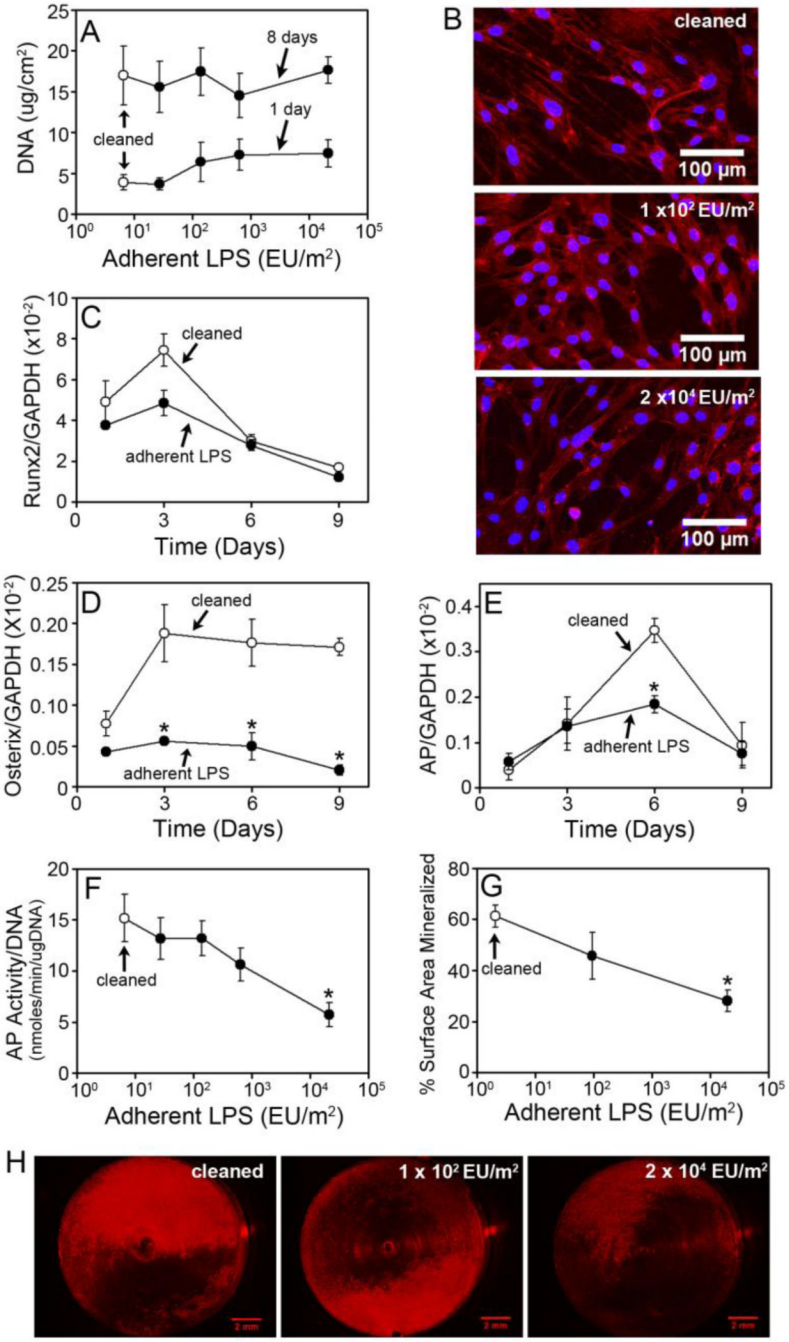

Figure 5. Adherent LPS inhibits osteoblast differentiation and mineralization in vitro

DNA measurements of MC3T3-E1 pre-osteoblast cells at one or eight days after plating on rigorously cleaned discs (open circles) or discs with adherent LPS (closed circles) (A). Fluorescent microscopic images of cells stained with Texas Red X phalloidin and DAPI on rigorously cleaned discs or discs with adherent LPS at one day in culture (B). Images are representative based on microscopic analysis of discs. Expression of runx2 (C), osterix (D) and alkaline phosphatase (E) normalized to GAPDH on rigorously cleaned discs (open circles) or discs with 2.7×10^4 EU/m^2 of adherent LPS (closed circles). Alkaline phosphatase activity at eight days in culture on rigorously cleaned discs (open circle) or discs with adherent LPS (closed circles) (F). The percentage of surface area mineralized as

assessed by xylenol orange staining at thirty days in culture on rigorously cleaned discs (open circles) or discs with adherent LPS (closed circles) (G). Representative rigorously cleaned discs and discs with adherent LPS, which are closest to the mean in G (H). Statistical analysis was by Two-Way ANOVA, * denotes $p<0.05$ compared to rigorously cleaned. Each data point represents the mean ± SEM of three to four independent experiments containing three to four discs per group, each assayed in triplicate (A, C–F), viewed using fluorescence microscopy (B), or analyzed for the percent of surface area mineralized (G).